Physics

Electricity & Magnetism fields

Okayama University *Year* 1991

Comparison of various methods of analysis and finite elements in 3-D magnetic field analysis

Takayoshi Nakata* N. Takahashi† K. Fujiwara‡
T. Imai** Kazuhiro Muramatsu††

*Okayama University
†Okayama University
‡Okayama University
**Okayama University
††ALPS Electric Company Limited, Miyagi

COMPARISON OF VARIOUS METHODS OF ANALYSIS AND FINITE ELEMENTS IN 3-D MAGNETIC FIELD ANALYSIS

T.Nakata*, N.Takahashi*, K.Fujiwara*, T.Imai* and K.Muramatsu**

* Dept. of Elec. Eng., Okayama University, Okayama, Japan
**Central Lab., ALPS Electric Co., Ltd., Kakuda, Japan

Abstract - In order to evaluate the most suitable method of analysis (A-ϕ or T-Ω method) and finite element (nodal or edge element) for a given problem, features of each method and element have been investigated. The accuracy, the computer storage and the CPU time of each method and element are compared with each other for the 3-D non-linear magnetostatic model (TEAM Workshop Problem 13) and the 3-D eddy current model (IEEJ model). The flux and eddy current densities calculated are compared with those measured.

It is shown that the accuracy and the CPU time of the edge element are better than those of the nodal element. The A method is better than Ω method for non-linear problems from the viewpoint of convergence characteristics of non-linear iterations.

1. INTRODUCTION

Various methods such as the A-ϕ and T-Ω methods[1-3], and various types of elements such as nodal and edge elements[3] have been used for 3-D magnetic field analysis. In order to decide the most suitable method of analysis and element for a given problem, the advantages and disadvantages of respective methods should be examined.

Although we already compared the accuracy, the computer storage and the CPU time for various methods of analysis and various types of elements[1-3], only linear eddy current problems were investigated, and various methods of analysis and various types of elements are not examined in detail. Therefore, we did not have enough information to decide favorable method and element for non-linear analysis. It is also not clear, even in a linear case, what kinds of method and element should be combined for a given problem.

In this paper, features of various methods (A-ϕ and T-Ω) and elements (1st-order brick nodal and edge) have been investigated systematically by analyzing the 3-D non-linear magnetostatic model[4] and the linear eddy current model[5]. Convergence characteristics of the Newton-Raphson iterations for various methods of analysis are also examined. Experiments are carried out to verify the accuracy.

2. ANALYSIS OF NON-LINEAR MAGNETIC FIELD (PROBLEM 13)

2.1 Description of Model

Figure 1 shows a 3-D non-linear magnetostatic model. Requirements in selecting such a model are described in the reference[4]. The coil is excited by dc currents. The ampere turns are 1000AT and 3000AT (which is sufficient to saturate the steel parts).

2.2 Numerical Analysis

The A and Ω methods using the 1st-order nodal and edge brick elements are used in the analysis. No gauge condition is imposed in all methods.

(1) Non-linear analysis

The modified Newton-Raphson method is used in non-linear analysis. In this method, the approximate potential $\{u\}^{(k+1)}$ obtained at the (k+1)-th iteration is given by the following equation:

$$\{u\}^{(k+1)} = \{u\}^{(k)} + \alpha \cdot \{\delta u\}^{(k)} \qquad (1)$$

where $\{\delta u\}$ are increments of the potentials, and α is a relaxation factor. In order to reduce the CPU time for solving linear equations, the convergence criterion ε_1 of the ICCG method can be chosen to be relatively large at earlier iterations[4]. ε_1 is chosen to 0.1 during the iterations at $\delta Bm > 0.1T$ (δBm : the maximum absolute value of the increment of flux density), and 10^{-5} at $\delta Bm < 0.1T$. The Newton-Raphson iteration is stopped when all the increments become less than 0.01T.

(2) Periodic boundary condition

Figure 2 shows the flux density vectors and the

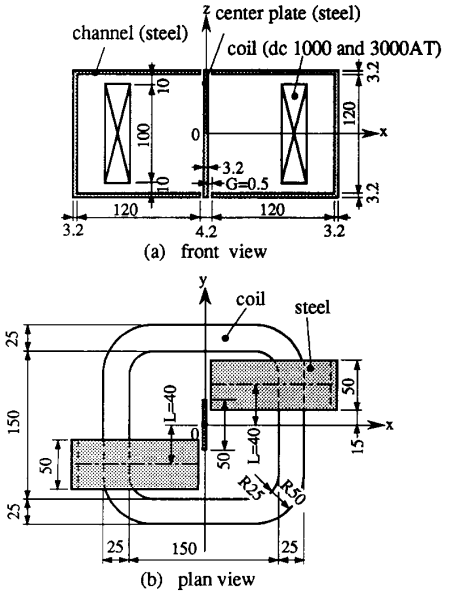

Fig. 1 3-D non-linear magnetostatic model.

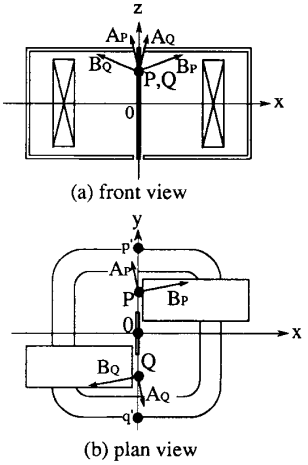

Fig. 2 Flux and potential distributions satisfying periodic condition.

magnetic vector potentials at the corresponding points P and Q on the periodic boundaries O-p' and O-q'. The flux densities B_P and B_Q at the points P and Q satisfy the following equations:

$$B_{Px} = -B_{Qx} \quad (2), \quad B_{Py} = -B_{Qy} \quad (3), \quad B_{Pz} = B_{Qz} \quad (4)$$

If such a periodic boundary condition[6] is applied, the region to be analyzed can be reduced to 1/4 of the whole region. As the relationship between the magnetic vector potentials A_P and A_Q at the points P and Q is the same as that between B_P and B_Q as shown in Fig.2, the periodic boundary condition of A for the nodal element is represented by the following equations:

$$A_{Px} = -A_{Qx} \quad (5), \quad A_{Py} = -A_{Qy} \quad (6), \quad A_{Pz} = A_{Qz} \quad (7)$$

As Eq.(5) corresponding to the x-component of A, which is normal to the boundary, cannot be taken into account by the edge element on the periodic boundaries O-p' and O-q' (y-z plane) shown in Fig.2, only Eqs.(6) and (7) are introduced when the edge element is used.

The periodic boundary condition of Ω is also obtained as follows:

$$\Omega_P = \Omega_Q \quad (8)$$

The analyzed region is subdivided into 1st-order brick elements. Figure 3 shows the mesh of the channel, the center plate and the coil. In order to subdivide

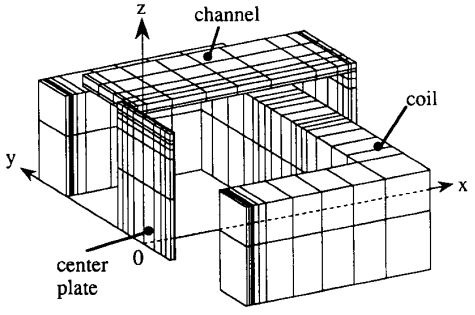

Fig. 3 Mesh of channel, center plate and coil.

the coil using only brick elements, the shape of the coil is modified so that the corner of the coil forms 90° edge as shown in Fig.3. The error due to the change of the shape is negligibly small[3].

2.3 Experiments

The channels and the center plate were annealed and demagnetized before the experiments. The average flux densities in the channels and the center plate are measured using one turn search coils as shown in Fig.4. The three components of flux densities in the air are measured using a 3-D Hall probe (F.W.BELL Co., type:ZOB1-3208). Its accuracy is within 1% and the active area is ϕ1.52mm. In order to guarantee the reproducibility of the measurement, a 3-D manipulator

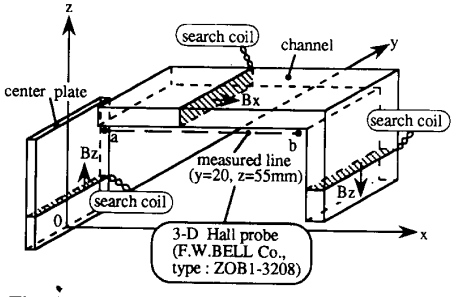

Fig. 4 Specified positions for comparing flux densities.

which can control the position of the probe within 0.1mm[7] is used.

2.4 Comparison and Discussion

Figure 5 shows the variations of the x-component Bsx of the flux density at the point S (near the edge of the channel) with the iteration number k. The point S is chosen, because the calculation error may occur at this point due to the quick change of flux density. Although the flux densities obtained by the A method using nodal and edge elements are converged smoothly, those by the Ω method become strongly oscillatory when α=1 in Eq.(1). The convergence characteristics of the Ω method can be improved by introducing the relaxation factor of α=0.5 as shown in Fig.5(b). For simplicity, α for all unknown potentials are chosen as the same values. In the above-mentioned investigation, the convergence criterion ε_I of the ICCG method is chosen to 10^{-5}.

Figure 6 shows the comparison of flux distributions using various methods. Figure (a) shows the average flux densities in the steel plates. Although there is a large discrepancy between the results calculated using the nodal element and results measured at 1000AT, the results calculated using the edge element is almost the same as the results measured. At 3000AT, however, the discrepancies between calculations using both types of elements and experiments are small due to the saturation of the steel. Figure (b) shows the absolute value |B| of flux density along the line a-b (y=20mm, z=55mm) in the air. The discrepancy of the flux density in the air is smaller than that in the steel plates.

The computer storage, the CPU time, etc. are shown

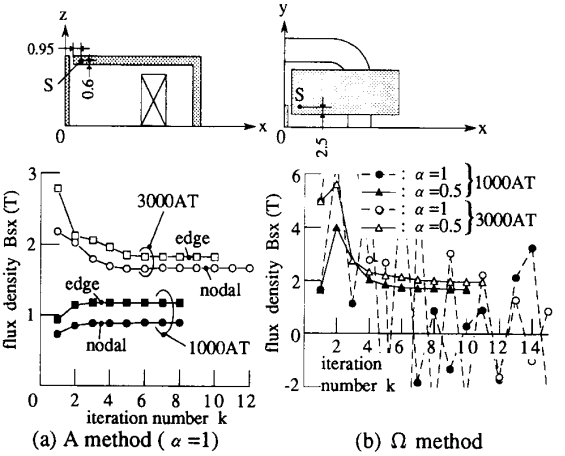

(a) A method (α =1) (b) Ω method

Fig. 5 Convergence characteristics of Newton-Raphson method ($\varepsilon_I = 10^{-5}$).

Table 1 Discretization data and CPU time (Problem 13)

item	A method				Ω method	
	nodal		edge		nodal	
ampere turn (AT)	1000	3000	1000	3000	1000	3000
number of elements	3564					
number of nodes	4370					
number of unknowns	9,550		10,080		2,944	
number of non-zero entries	340,075		155,074		36,012	
computer storage (MB)	8.0		4.0		1.6	
number of iterations of Newton-Raphson method	8 (4)	12 (7)	9(3)	10(7)	10 (7)	13 (8)
CPU time(s)	1929	2608	293	219	75	118

computer used : NEC supercomputer SX-1E
(maximum speed : 285MFLOPS)
(n) : number of iterations until $|\delta B|_m$ becomes less than 0.1T.

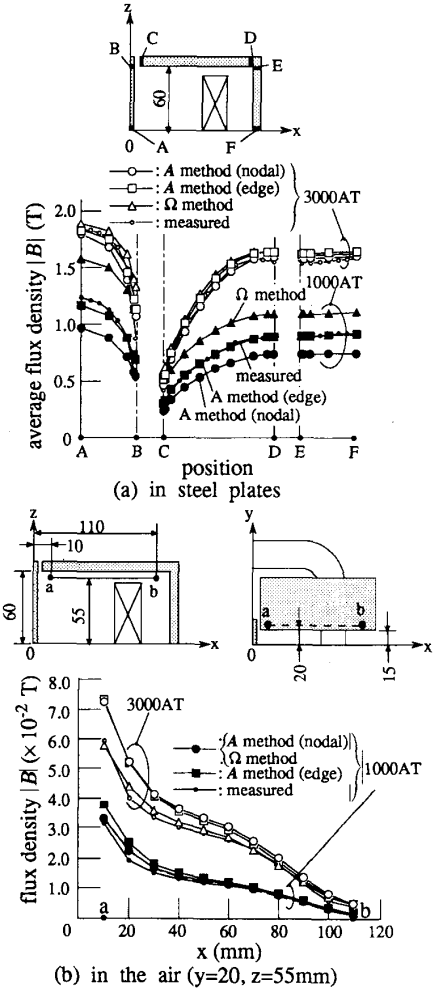

Fig. 6 Comparison of flux distributions.

in Table 1. Although the number of iterations of the Newton-Raphson method for the Ω method is greater than that for the A method, the CPU time for the Ω method is much smaller than that for the A method. Although the number of unknown variables for the A method with nodal element is almost the same as that for the A method with edge element, the computer storage and the CPU time for the edge element is about 1/2 and 1/10 respectively, compared with those for the nodal element. This is, because the number of non-zero entries of the coefficient matrix for the edge element is much less than that for the nodal element.

3. ANALYSIS OF MAGNETIC FIELD WITH EDDY CURRENT (IEEJ MODEL)

3.1 Description of Model

Figure 7 shows a model proposed by the IEE of Japan. The features of the model are described in the reference[5]. A rectangular ferrite core is surrounded by an exciting coil. An ac current of which the effective value is 1000AT (frequency: 50Hz) is applied. Two aluminum plates are set on the upper and lower sides of the core. The conductivity of the aluminum is equal to 3.215×10^7S/m, and the relative permeability (μ_r) of the core is assumed to be 3000. Both cases with and without hole in the plates are investigated.

3.2 Numerical Analysis

The A-ϕ and T-Ω methods with nodal and edge elements are applied. The electric scalar potential ϕ is set at zero in the A-ϕ method with edge element. In the T-Ω method, the conductivity of the hole is assumed to 1S/m[8]. 1/8 region is analyzed.

3.3 Experiments

There exists induction of noise in magnetic field at the junction between the Hall sensor and lead wires, because the sufficient twisting of conductors is difficult. Therefore, the flux density is measured using a small search coil with 20 turns (mean diameter: 3mm, height: 0.6mm, conductor diameter: 0.06mm).

The eddy current density on the surface of the aluminum plate is measured using the modified probe method[9], and the total eddy current is measured by a Rogowski coil.

3.4 Comparison and Discussion

Figure 8 shows the maximum absolute value |B| of the flux density along the line at z=57.5mm. Figure 9

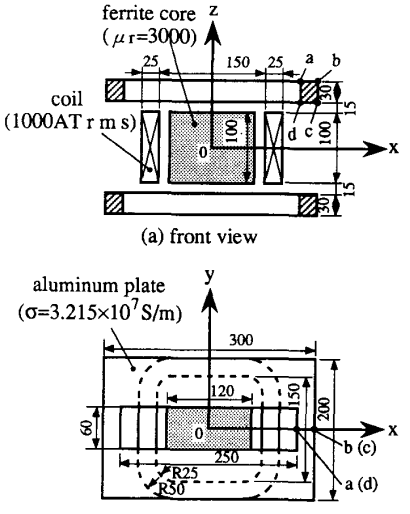

Fig.7 Analyzed model (with hole).

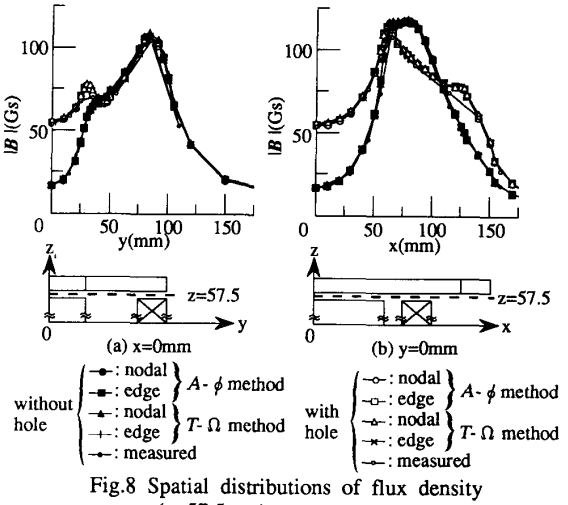

Fig.8 Spatial distributions of flux density (z=57.5mm).

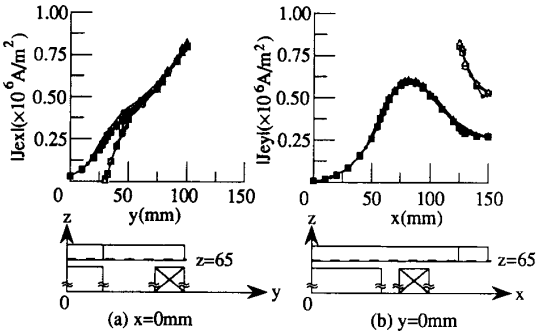

Fig.9 Spatial distribution of eddy current density (z=65mm).

Table 2 Comparison of eddy current (with hole)

item	$A-\phi$		$T-\Omega$		measured
	nodal	edge	nodal	edge	
amplitude of eddy current |Ie| (A)	317	319	318	318	313
error ε (%)	1.28	1.92	1.60	1.60	——

shows the x-component |Jex| of the effective value of the eddy current density on the surface (z=65mm) of the aluminum plate. The results calculated usirg various methods and elements and results measured are almost the same. Table 2 shows the comparison of calculated and measured values of total eddy current Ie passing through at the cross section a-b-c-d-a in Fig.7. The error ε is defined by

$$\varepsilon = \left| \frac{Ie(cal)-Ie(mea)}{Ie(mea)} \right| \times 100\ (\%) \qquad (9)$$

where Ie(cal) is the current calculated and Ie(mea) is the current measured.

The computer storage, the CPU time, etc. are shown in Table 3. The CPU time for the $T-\Omega$ method in the analysis of the model without hole is extremely decreased compared with the $A-\phi$ method. The CPU times for the $A-\phi$ and $T-\Omega$ methods with edge element are about 1/6 and 1/2 of those with nodal element. Although the CPU time for the $T-\Omega$ method in the analysis of the model with hole is rapidly increased compared with that without hole in the case of nodal element, it is not so remarkable in the case of edge element. From the viewpoint of the CPU time, the $T-\Omega$ method with edge element is favorable.

Table 3 Discretization data and CPU time

item	without hole				with hole			
	$A-\phi$		$T-\Omega$		$A-\phi$		$T-\Omega$	
	nodal	edge	nodal	edge	nodal	edge	nodal	edge
number of elements	14400							
number of nodes	16275							
number of unknowns	43417	41060	22844	22412	42885	41060	22844	22412
number of non-zero entries	1781644	653718	632859	423056	1734684	653718	632859	423056
computer storage (MB)	72.2	28.4	30.7	19.4	70.5	28.4	30.7	19.4
number of iterations of ICCG method	1306	513	172	192	1264	582	1141	327
CPU time (s)	6242	947	533	290	5870	1069	2001	442

Computer used : NEC supercomputer SX-1E
(maximum speed : 285 MFLOPS)
convergence criterion of ICCG method : 10^{-7}

4. CONCLUSIONS

The features of various methods ($A-\phi$ and $T-\Omega$) and elements (nodal and edge) have been investigated by analyzing the 3-D non-linear magnetostatic model and the eddy current model. The results obtained can be summarized as follows:

(1) In the case of the non-linear magnetostatic model (Problem 13), the most accurate results are obtained using the A method with edge element.
(2) In the non-linear analysis, the convergence of the Newton-Raphson iterations for the Ω method is not as fast as that for the A method. It can be improved by introducing the relaxation factor.
(3) Although the CPU time for the $T-\Omega$ method using nodal element is rapidly increased when there exists a hole (IEEJ model), the rate of increase of the CPU time is not so remarkable if the edge element is used.
(4) The accuracy and the CPU time for the edge element are better than those for the nodal element. From the viewpoint of the CPU time, the $T-\Omega$ method is favorable, and from the viewpoint of the accuracy, the $A-\phi$ method is favorable.

It is necessary to examine the above-mentioned features of various methods of analysis and finite elements by applying them to systematically conceived models in order to obtain universal descriptions of the features. The systematic investigation will be reported in another paper.

ACKNOWLEDGMENT

This work was partly supported by the Grant-in-Aid for Co-operative Research (A) from the Ministry of Education, Science and Culture in Japan (No.01302031).

REFERENCES

[1] T.Nakata, N.Takahashi, K.Fujiwara, K.Muramatsu and Z.G. Cheng: "Comparison of Various Methods for 3-D Eddy Current Analysis", IEEE Trans. on Magnetics, MAG-24, 6, 3159 (1988).
[2] T.Nakata, N.Takahashi, K.Fujiwara and K.Muramatsu: "Investigation of Effectiveness of Various Methods with Different Unknown Variables for 3-D Eddy Current Analysis", ibid., MAG-26, 2, 442 (1990).
[3] T.Nakata, N.Takahashi, K.Fujiwara and Y.Shiraki: "Comparison of Different Finite Elements for 3-D Eddy Current Analysis", ibid., MAG-26, 2, 434 (1990).
[4] T.Nakata, N.Takahashi, K.Fujiwara, P.Olszewski and K.Muramatsu: "Analysis of Magnetic Fields of 3-D Non-Linear Magnetostatic Model (PROBLEM 13)", Proc. of European TEAM Workshop and International Seminar on Electromagnetic Field Analysis, Oxford, 107 (1990).
[5] T.Nakata, N.Takahashi, K.Fujiwara and P.Olszewski: "Verification of Softwares for 3-D Eddy Current Analysis using IEEJ Model", Advances in Electrical Engineering Software (Ed. P.P.Silvester), 349 (1990) Springer-Verlag.
[6] T.Nakata, N.Takahashi, K.Fujiwara and A.Ahagon: "Periodic Boundary Condition for 3-D Magnetic Field Analysis and Its Applications to Electrical Machines", IEEE Trans. Magnetics, MAG-24, 6, 2694 (1988).
[7] J.Takehara, M.Kitagawa, T.Nakata and N.Takahashi: "Finite Element Analysis of Inrush Currents in Three-Phase Transformers", ibid., MAG-23, 5, 2647 (1987).
[8] T.Nakata, N.Takahashi, K.Fujiwara and Y.Okada: "Improvement of $T-\Omega$ method for 3-D Eddy Current Analysis", ibid., MAG-24, 1, 94 (1987).
[9] T.Nakata, K.Fujiwara, M.Nakano and T.Kayada: "Effects of the Construction of Yokes on the Accuracy of a Single Sheet Tester", Anales de Fisica, B, 86, 190 (1990).